HNPS Advances in Nuclear Physics

Neutrino masses and interactions from Super-Kamiokande

S. Lola

Neutrino masses and interactions from Super-Kamiokande

Smaragda Lola

CERN Theory Division, CH-1211 Geneva 23, Switzerland

Abstract

We discuss topics on neutrino masses and interactions, in the light of the Super-Kamiokande data. The experimental observations can be explained either by several patterns of neutrino masses, or by flavour-changing neutrino matter-interactions. In the latter case, the coupling constants of the relevant operators are large enough to give interesting signals in ultra-high energy neutrino scattering to matter.

1   Neutrino data and Implications

Recent reports by Super-Kamiokande [1] and other experiments [2] support previous measurements of a ν_μ/ν_e ratio in the atmosphere, which is significantly smaller than the theoretical expectations. The data favours ν_μ–ν_τ oscillations, with

$$\delta m^2_{\nu_\mu \nu_\tau} \approx (10^{-2} \text{ to } 10^{-3}) \text{ eV}^2 \tag{1}$$

$$\sin^2 2\theta_{\mu\tau} \geq 0.8 \tag{2}$$

On the other hand, the solar neutrino puzzle can be resolved through either vacuum or matter-enhanced (MSW) oscillations. The first require a mass splitting of the neutrinos that are involved in the oscillations in the range $\delta m^2_{\nu_e \nu_\alpha} \approx (0.5 - 1.1) \times 10^{-10}$ eV^2, where α is μ or τ. MSW oscillations allow for both small and large mixing, while now $\delta m^2_{\nu_e \nu_\alpha} \approx (0.3 - 20) \times 10^{-5}$ eV^2. Moreover, the LSND collaboration has reported evidence for the appearance of $\bar{\nu}_\mu$–$\bar{\nu}_e$ and ν_μ–ν_e oscillations [3], which are not, however, supported by KARMEN 2 [4]. Finally, if neutrinos were to provide a hot dark matter component, then the heavier neutrino(s) should have mass in the range $\sim (1 - 6)$ eV.

The simplest class of solutions that one may envisage, in order to accommodate the neutrino data, consists of an extension of the Standard Model to include

three right-handed neutrino states, with a mass structure directly related to that of the other fermions. Three neutrino masses allow only two independent mass differences and thus the direct indications for neutrino oscillations discussed above cannot be simultaneously explained, unless a sterile light neutrino state is introduced. Since the LSND results have not been confirmed, in our analysis we chose not to introduce sterile states (which inevitably break any simple connection of the neutrino masses with the known charged lepton and quark hierarchies). Instead, we focus on the Super-Kamiokande and the solar neutrino data, and leave open the possibility of neutrinos as hot dark matter. In this framework, both the solar and atmospheric deficits require small mass differences, and can thus be explained by two possible neutrino hierarchies:

(a) Textures with almost degenerate neutrino eigenstates, with mass $\mathcal{O}(\text{eV})$. In this case neutrinos may also provide a component of hot dark matter.

(b) Textures with large hierarchies of neutrino masses: $m_3 g^2 m_2, m_1$, with the possibility of a second hierarchy $m_2 g^2 m_1$. Then, the atmospheric neutrino data would require $m_3 \approx (10^{-1} \text{ to } 10^{-1.5})$ eV and $m_2 \approx (10^{-2} \text{ to } 10^{-3})$ eV.

A natural question that then arises is why neutrino masses are smaller that the rest of the fermion masses in the theory. This can be explained by the see-saw mechanism [5]. Suppose that $M_{\nu_L} = \nu_L \nu_L$ is zero to start with. Still, a naturally small effective Majorana mass for the light neutrinos (predominantly ν_L) can be generated by mixing them with the heavy states (predominantly ν_R) of mass M_{ν_R}. In this case, the light eigenvalues of the mass matrix $M = \begin{pmatrix} 0 & m_\nu^D \\ m_\nu^{D^T} & M_{\nu_R} \end{pmatrix}$ are contained in $m_{light} \simeq \frac{(m_\nu^D)^2}{M_{\nu_R}}$, where m_ν^D is the Dirac neutrino mass matrix, and are naturally suppressed. Then, the neutrino data clearly constrain the possible mass scales of the problem. For a scale $\mathcal{O}(200 \text{ GeV})$, solutions of the type (a) (that is light neutrinos of almost equal mass), require $M_{N_3} \approx \mathcal{O}(\text{a few times } 10^{13} \text{ GeV})$. On the other hand, solutions of the type (b), with large light neutrino hierarchies require $M_{N_3} \approx O(\text{a few times } 10^{14} - 10^{15} \text{ GeV})$.

2   Phenomenological Textures

We can now try to understand in more detail the neutrino mass structure that may account for the various deficits. The fact that fermion mass matrices exhibit a hierarchical structure suggests that they are generated by an underlying family symmetry [6,7], although here we will study phenomenological textures, without referring to the underlying mechanism that generates them (we will follow the lines of [8], however the results are also overlapping with those in the recent literature [9]). Let us start with the light-neutrino

mass matrix, in the basis where the charged leptons are diagonal. This may be written as

$$m_{eff} = m_\nu^D \cdot (M_{\nu_R})^{-1} \cdot m_\nu^{D^T} \tag{3}$$

To identify which mass patterns may fulfill the phenomenological requirements outlined in the previous section, we concentrate initially on the 2×2 mass submatrix for the second and third generations. Then one can write:

$$m_{eff}^{-1} = V_\nu m_{eff}^{-1\ diag} V_\nu^T, \quad m_{eff}^{-1\ diag} = \begin{pmatrix} \frac{1}{m_2} & 0 \\ 0 & \frac{1}{m_3} \end{pmatrix} \tag{4}$$

where we are going to explore large (2–3) mixing. For $V_\nu = \begin{pmatrix} c_{23} & -s_{23} \\ s_{23} & c_{23} \end{pmatrix}$, m_{eff}^{-1} takes the form

$$m_{eff}^{-1} \equiv d \begin{pmatrix} b/d & 1 \\ 1 & c/d \end{pmatrix} = \frac{1}{m_2 m_3} \begin{pmatrix} c_{23}^2 m_3 + s_{23}^2 m_2 & c_{23} s_{23}(m_3 - m_2) \\ c_{23} s_{23}(m_3 - m_2) & c_{23}^2 m_2 + s_{23}^2 m_3 \end{pmatrix} \tag{5}$$

The mass eigenvalues $m_{2,3}$ are given by

$$m_{2,3} = \frac{2}{b + c \pm \sqrt{(b-c)^2 + 4d^2}} \tag{6}$$

while the $\nu_\mu - \nu_\tau$ mixing angle is defined as

$$\sin^2 2\theta_{23} = \left(2d \frac{m_2 m_3}{m_3 - m_2}\right)^2 = \frac{4d^2}{(b-c)^2 + 4d^2} \tag{7}$$

Maximal mixing: $\sin^2 2\theta_{23} \approx 1$, $\theta_{23} \approx \pi/4$ is obtained whenever $|b - c| \ll |d|$. Concerning the mass hierarchies, one sees the following: if the diagonal or the off-diagonal entries dominate, the neutrino mass hierarchies are small. On the other hand, if all entries are of the same order, large hierarchies are generated.

Having commented on the possible structure of m_{eff}, the next question is: From what forms of Dirac and heavy Majorana mass structures may we obtain the desired m_{eff}? The form of the heavy Majorana mass matrix M_{ν_R} may easily be found from $M_{\nu_R} = m_\nu^{D^T} \cdot m_{eff}^{-1} \cdot m_\nu^D$ once the neutrino Dirac mass

Table 1

Approximate forms for some of the basic structures of symmetric textures, keeping the dominant contributions.

m_ν^D	$m_\nu^{D,diag}$	M_{ν_R}	$M_{\nu_R}^{diag}$
$\begin{pmatrix} \lambda & \lambda^2 \\ \lambda^2 & 1 \end{pmatrix}$	$\begin{pmatrix} \lambda & 0 \\ 0 & 1 \end{pmatrix}$	$\begin{pmatrix} 2\lambda^2 & 1 \\ 1 & 2\lambda \end{pmatrix}$	$\begin{pmatrix} -1 & 0 \\ 0 & 1 \end{pmatrix}$
$\begin{pmatrix} \lambda^3 & \lambda^2 \\ \lambda^2 & 1 \end{pmatrix}$	$\begin{pmatrix} \lambda^3 & 0 \\ 0 & 1 \end{pmatrix}$	$\begin{pmatrix} 2\lambda^3 & \lambda \\ \lambda & 2 \end{pmatrix}$	$\begin{pmatrix} -\frac{\lambda^2}{2} & 0 \\ 0 & 2 \end{pmatrix}$
$\begin{pmatrix} \lambda & 1 \\ 1 & \lambda \end{pmatrix}$	$\begin{pmatrix} -1 & 0 \\ 0 & 1 \end{pmatrix}$	$\begin{pmatrix} 2\lambda & 1 \\ 1 & 2\lambda \end{pmatrix}$	$\begin{pmatrix} -1 & 0 \\ 0 & 1 \end{pmatrix}$

matrix has been specified. It is clear that if the neutrino Dirac mass matrix is diagonal, one particular solution is

$$M_{\nu_R} \propto (M_{\nu_R})^{-1} \propto m_{eff} \propto \begin{pmatrix} 0 & 1 \\ 1 & 0 \end{pmatrix} \tag{8}$$

which we discussed in detail in [10]. Of course, as the Dirac mass matrix changes, different forms of M_{ν_R} are required in order to obtain the desired form of m_{eff}. This is exemplified in Table 1, where we show the textures that lead to m_{eff} as given in (8) for three different mixing parameters in the Dirac mass matrix [8].

The above can be described in a more generic way: for simplicity, we consider the case of a symmetric Dirac mass matrix with mixing angle ϑ. We define ϕ to be the mixing angle in the heavy Majorana neutrino mass matrix, and denote by θ the resulting mixing angle in the light-neutrino mass matrix m_{eff} (where from now on we drop the sub-indices that refer to the (2–3) sector). Then, the mixing angle in M_{ν_R} can be expressed as [8]

$$\tan 2\phi = \frac{\sin(4\vartheta - 2\theta) + r^2 \sin 2\theta - 2rR \sin 2\vartheta}{\cos(4\vartheta - 2\theta) + r^2 \cos 2\theta - 2rR \cos 2\vartheta} \tag{9}$$

Here, M_3 and M_2 are the eigenvalues of the heavy Majorana mass matrix, $R \equiv (m_2 + m_3)/(m_3 - m_2)$ with m_i being the eigenvalues of the light-neutrino mass matrix, and $r \equiv (m_2^D + m_3^D)/(m_3^D - m_2^D)$, with the m_i^D being the eigenvalues of the Dirac mass matrix. This equation relates the mass and mixing parameters of the various neutrino sectors.

The 2×2 description may be a good approximation in the limit where the solar neutrino problem is resolved by a small mixing angle. However, this need not

be the case, and one should consider the 3×3 mixing problem, with a mixing matrix $V_{3 \times 3}(\theta_{12}, \theta_{23}, \theta_{13})$. Investigating the possible hierarchies within m_{eff} is then straightforward, since it is given by $m_{eff} = V_{3 \times 3} . m_{eff}^{diag} . V_{3 \times 3}^{\dagger}$. When specific limits are considered, simple expressions for m_{eff} can be derived. For example, for maximal θ_{12}, θ_{23} mixing and $\theta_{13} \sim 0$, in the limit $m_3 g^2 m_2 g^2 m_1$, one has:

$$
m_{eff} = \frac{m_3}{2} \begin{pmatrix} 0 & 0 & 0 \\ 0 & 1 & -1 \\ 0 & -1 & 1 \end{pmatrix} + \frac{m_2}{2} \begin{pmatrix} 1 & -\frac{1}{\sqrt{2}} & -\frac{1}{\sqrt{2}} \\ -\frac{1}{\sqrt{2}} & \frac{1}{2} & \frac{1}{2} \\ -\frac{1}{\sqrt{2}} & \frac{1}{2} & \frac{1}{2} \end{pmatrix} + \frac{m_1}{2} \begin{pmatrix} 1 & \frac{1}{\sqrt{2}} & \frac{1}{\sqrt{2}} \\ \frac{1}{\sqrt{2}} & \frac{1}{2} & \frac{1}{2} \\ \frac{1}{\sqrt{2}} & \frac{1}{2} & \frac{1}{2} \end{pmatrix}
$$

Analogous expressions are obtained in the case where the neutrino masses exhibit some degeneracy.

What about the structure of the Dirac and heavy Majorana matrices that generate viable m_{eff}'s in this case? In view of the many parameters, at this stage we look at some limiting cases for symmetric Dirac mass matrices (subsequently we will examine solutions in models with flavour symmetries, including also asymmetric textures). It is convenient to parametrize the output in terms of the hierarchy factors $x \equiv m_1/m_3, y \equiv m_2/m_3$ for the ratios of eigenvalues of m_{eff} and $\lambda_1 \equiv m_{\nu_1}^D/m_{\nu_3}^D, \lambda_2 \equiv m_{\nu_2}^D/m_{\nu_3}^D$ for the ratios of eigenvalues of the neutrino Dirac mass matrix m_ν^D.

(A) We can distinguish two cases for the structure of the heavy Majorana matrix: the first is that of *matched mixing*, which occurs when we have one large mixing angle in the (2–3) sector of m_{eff} and there is no large mixing in other sectors of either the light Majorana or the Dirac matrices. In this case, the problem is equivalent to the 2×2 case considered previously. In the particular cases where $y = m_2/m_3 = -1$ and $x \ll y \ll 1$, one obtains the textures

$$
M_{\nu_R} \propto \begin{pmatrix} \frac{\lambda_1^2}{x} & 0 & 0 \\ 0 & 0 & \lambda_2 \\ 0 & \lambda_2 & 0 \end{pmatrix}, \quad M_{\nu_R} \propto \begin{pmatrix} \frac{\lambda_1^2}{x} & 0 & 0 \\ 0 & \frac{\lambda_2^2}{2y} & \frac{\lambda_2}{2y} \\ 0 & \frac{\lambda_2}{2y} & \frac{1}{2y} \end{pmatrix} \tag{10}
$$

respectively, which indicates the decoupling of the light sector.

(B) A different structure arises when (i) there is more than one mixing angle in m_{eff} and/or (ii) there is a large Dirac mixing angle that involves different generations from those of the light Majorana matrix. This happens, for example, when the atmospheric problem is solved by $\nu_\mu \to \nu_\tau$ oscillations, whilst the Dirac mass matrix is related to the quark mass matrix, with Cabibbo mix-

ing between the first and second generations. The structure of the Majorana matrix becomes more complicated for this *mismatched mixing*. It is interesting to note that, for an almost-diagonal Dirac mass matrix and large Dirac hierarchies (and in particular $\lambda_1 \ll \lambda_2$), the light entry of the heavy Majorana mass matrix again effectively decouples from the heavier ones [8]. This is no longer true, however, if the (12) mixing angle in the Dirac mass matrix increases. For example, for maximal (1–2) Dirac mixing (which is plausible, as we discuss below), two large mixing angles in m_{eff} (θ_{23} and θ_{12}), and large hierarchies $y \ll 1$ and $\lambda_2^2 x g^2 \lambda_1^2 y$, one has

$$
M_{\nu_R} \propto \frac{1}{2y} \times \begin{pmatrix} \frac{\lambda_2^2}{2} & \frac{\lambda_2^2}{2} & \frac{-\lambda_2}{\sqrt{2}} \\ \frac{\lambda_2^2}{2} & \frac{\lambda_2^2}{2} & \frac{-\lambda_2}{\sqrt{2}} \\ \frac{-\lambda_2}{\sqrt{2}} & \frac{-\lambda_2}{\sqrt{2}} & 1 \end{pmatrix}
\tag{11}
$$

while for intermediate (1–2) Dirac mixing the effect lies between the two limiting cases that we discussed. Since there is a vast number of possibilities for the origin of proper mixings, we will investigate the type of constraints that may be obtained from flavour symmetries.

3   Lepton-number violation in Ultra-High-Energy neutrinos

Besides neutrino oscillations, alternative possibilities for explaining the atmospheric neutrino data have been discussed, such as neutrino decay [11] and flavour–changing neutrino–matter interactions [12]. The latter (which arise in many Standard Model extensions, such as R-violating supersymmetry and leptoquark models) had already been used in the past, for solar neutrino conversions. However, in recent proposals it has been shown that they may also account for the Super-Kamiokande observations, without directly discussing neutrino masses. The relevant process would be $\nu_\mu + f \to \nu_\tau + f$, where the required couplings are of the order of $\lambda_{\tau f} \cdot \lambda_{\mu f} \approx 0.1$, for propagators with masses of 200 GeV [12]. Then, the immediate question that arises is whether there is any way to directly probe such couplings. In this framework, it had already been pointed out that such couplings may induce significant changes in the interaction rates of ultra-high energy neutrinos (UHE) with nucleons and electrons, through the production of particle resonances [13].

To make the analysis more specific, we will discuss lepton-number violation in the framework of R-violating SUSY, however, the results are more generic. In these models the lepton-number violating operators that are consistent with

Table 2

Experimental constraints (at one or two standard deviations) on the R-violating Yukawa couplings of interest, for the case of 200-GeV sfermions. For arbitrary sfermion mass the limits scale as by $(m_{\tilde{f}}/200$ GeV$)$, except for λ'_{221}.

Coupling	Limited by
$\lambda_{12k} < 0.1\ (2\sigma)$	CC universality
$\lambda_{131,132,231} < 0.12\ (1\sigma)$	$\Gamma(\tau \to e\nu\bar{\nu})/\Gamma(\tau \to \mu\nu\bar{\nu})$
$\lambda_{133} < 0.006\ (1\sigma)$	ν_e Majorana mass
$\lambda'_{21k} < 0.18\ (1\sigma)$	π decay
$\lambda'_{221} < 0.36\ (1\sigma)$	D decay
$\lambda'_{231} < 0.44\ (2\sigma)$	ν_μ deep inelast. scatter.

the symmetries of the theory are

$$W_{\Delta L \neq 0} = \lambda_{ijk} L^i L^j \overline{E}^k + \lambda'_{ijk} L^i Q^j \overline{D}^k \tag{12}$$

where i, j, k are generation indices; $L^i \equiv (\nu^i, e^i)_{\mathrm{L}}$ and $Q^i \equiv (u^i, d^i)_{\mathrm{L}}$ are the left-chiral superfields, and $\overline{E}^i \equiv e^i_{\mathrm{R}}$, $\overline{D}^i \equiv d^i_{\mathrm{R}}$, and $\overline{U}^i \equiv u^i_{\mathrm{R}}$ the right-chiral ones. The good agreement between the data and the standard-model expectations implies bounds on the strength of lepton-number-violating operators [14]. Then, the situation is the following: $LQ\overline{D}$-type interactions of electron neutrinos or antineutrinos with the first-generation quarks are highly constrained from various processes, such as neutrinoless double-beta decay, charged-current (CC) universality, atomic parity violation, and the decay rate of $K \to \pi\nu\bar{\nu}$. The bounds on $LL\overline{E}$ couplings are also strong. On the other hand, experimental limits on the $L^i Q^j \overline{D}^k$ couplings that involve ν_μ, which would be relevant to explaining the Super-Kamiokande data, are less restrictive. Some useful bounds in the case that one R-violating coupling dominates appear in Table 2.

UHE neutrinos are produced from the interactions of energetic protons in active galactic nuclei (AGN), as well as from gamma-ray bursters or pion photoproduction on the cosmic microwave background. Moreover, they may also arise from exotic heavy-particle decays and the collapse of topological defects. Their effects can be observed in neutrino telescopes [15] and it is important in this respect to look for specific signals of lepton-number violation as km³-class neutrino observatories come into being. The dominant mechanisms for

producing UHE photons and neutrinos are expected to be

$$p\,(p/\gamma) \to \pi^0 + \text{anything}$$
$$ \,\,\,\llcorner\,\, \gamma\gamma \qquad\qquad\qquad\qquad (13)$$

and

$$p\,(p/\gamma) \to \pi^\pm + \text{anything}$$
$$ \llcorner\,\, \mu\nu_\mu \qquad\qquad\qquad\qquad (14)$$
$$ \llcorner\,\, e\nu_e\nu_\mu\,.$$

If π^+, π^-, and π^0 are produced in equal numbers, the relative populations of neutral particles will be $2\gamma : 2\nu_\mu : 2\overline{\nu}_\mu : 1\nu_e : 1\overline{\nu}_e$. Since there are no significant conventional sources of ν_τ and $\overline{\nu}_\tau$, we are not able to probe lepton-number-violating operators of the $L_3Q\overline{D}$ type.

What is the effect of the new couplings? Let us first consider $\nu_\mu N$ interactions. The charged-current reaction $\nu_\mu N \to \mu^- +$ anything can receive contributions from (i) the s-channel process $\nu_\mu d_L \to \tilde{d}_R^k \to \mu_L^- u_L$, which involves valence quarks, and from (ii) u-channel exchange of $\tilde{d}_R^k$ in the reaction $\nu_\mu \overline{u} \to \overline{d}\mu^-$, which involves only sea quarks. As a consequence of the spread in quark momenta, the resonance peaks in case (i) are not narrow, but are broadened and shifted above the threshold energies. The right-handed squark $\tilde{d}_R^k$ has a similar influence on the neutral-current reaction $\nu_\mu N \to \nu_\mu +$ anything. On the other hand, left-handed squarks can contribute *only* to the neutral-current reaction and we therefore predict modifications to the ratio of neutral-current to charged-current interactions [13]. Similar effects are observed in $\overline{\nu}_\mu N$ interactions. In Fig.1, we compare the ratio $\sigma_{\rm NC}/\sigma_{\rm CC}$ in the standard model with the case where lepton-number-violating couplings are present. In this calculation, we use the CTEQ3 parton distributions [16]. Although neutrino telescopes will not distinguish between events induced by neutrinos and antineutrinos and the relevant quantity would thus be the sum of the $\nu_\mu N$ and $\overline{\nu}_\mu N$ cross sections, we present these processes separately in order to stress the effects of the helicity structure of the theory.

We see that the modifications from the Standard Model cross sections are appreciable, even away from the resonance bump.

What about neutrino interactions on electron targets? In the Standard Model, due to the smallness of the electron-mass, neutrino-electron interactions in matter are weaker than neutrino-nucleon interactions, with the exception of the resonant formation of the intermediate boson in $\overline{\nu}_e e \to W^-$ interactions
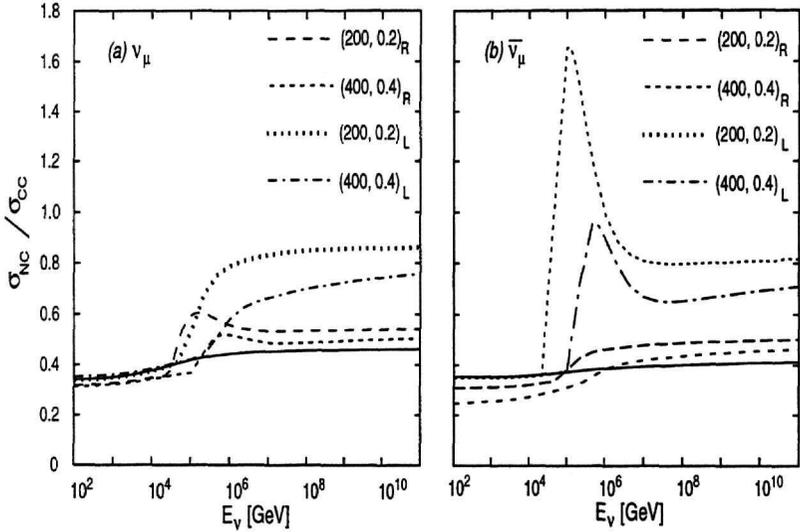
Fig. 1. *Neutral-current to charged-current ratios for (a) $\nu_\mu N$ and (b) $\bar{\nu}_\mu N$ inter-actions. The solid lines show the predictions of the standard model. The dashed (short-dashed) curves include the contributions of a right-handed squark, $\tilde{d}_R^k$, with mass $\tilde{m} = 200$ (400) GeV and coupling $\lambda'_{21k} = 0.2$ (0.4). The dotted (dot-dashed) curves include the contributions of a left-handed squark, $\tilde{d}_L^k$, for the same masses and couplings.*

[15]. Additional effects may arise through R-violating interactions [13]. Be-cause the $LL\overline{E}$ couplings are constrained to be small, only channels that in-volve resonant slepton production can display sizeable effects. Such couplings are too small to explain the Super-Kamiokande data in the framework of [12], nevertheless it is interesting to investigate whether they could have any ob-servable effect. Small couplings result in small decay widths, and consequently, it will be difficult to separate such a narrow structure from the standard-model background. One interesting characteristic is that the slepton resonance will only be produced in downward-going interactions. Indeed, in water-equivalent units, the interaction length is given by

$$L_{\text{int}}^{(e)} = \frac{1}{\sigma(E_\nu)(10/18)N_A} \qquad (15)$$

N_A is the Avogadro's number and $(10/18)N_A$ is the number of electrons in a mole of water. At the peak of a 200 or 400 GeV slepton resonance pro-duced in $\bar{\nu}e$ interactions, the interaction length indicates that the resonance is effectively extinguished for neutrinos that traverse the Earth.

Still, it would be easier to observe a slepton resonance in the case where the produced final states clearly stand out against the background. One such possibility arises if many R-violating couplings are simultaneously large, thus

leading to exotic final-state topologies. An even better possibility arises if neutralinos are relatively light. In this case, the slepton may also decay into the corresponding lepton and a light neutralino, which in its turn decays into leptons and neutrinos:

$$\nu_\mu e_L^- \to \tilde{\tau}_R^- \to \tau^- \tilde{\chi}^0$$
$$\quad\quad\quad\quad\quad \hookrightarrow \tau_R^+ \nu_e \mu_L^- \text{ or } \tau_R^+ \nu_\mu e_L^- \tag{16}$$

and

$$\overline{\nu_{e,\mu}} e_R^- \to \tilde{\tau}_L^- \to \to \tau^- \tilde{\chi}^0$$
$$\quad\quad\quad\quad\quad \hookrightarrow \tau_L^+ \overline{\nu} e_R^- \tag{17}$$

The decay length of a 1-PeV τ is about 50 m, so the production and subsequent decay of a τ at UHE will result in a characteristic "double-bang" signature in a Cherenkov detector. Because there are no conventional astrophysical sources of tau-neutrinos, while τ-production through a slepton resonance with a mass ≥ 200 GeV, is essentially background-free, reactions that produce final state τ-leptons are of special interest for probing new physics.

4 Summary and Conclusions

We discussed various aspects of neutrino masses and lepton number violation, in the light of the observations by Super-Kamiokande. We studied phenomenological neutrino mass textures which match the data from various experiments. However, we also have schemes where the neutrino data are explained simply by flavour-changing interactions. In this latter case, channels to directly search for lepton-number violation in ultra-high energy neutrino interactions, have also been proposed.

Acknowledgements

References

[1] Y. Fukuda et al., Super-Kamiokande collaboration, Phys. Lett. B433 (1998) 9; Phys. Lett. B436 (1998) 33; Phys. Rev. Lett. 81 (1998) 1562.

[2] S. Hatakeyama et al., Kamiokande collaboration, Phys. Rev. Lett. 81 (1998) 2016; M. Ambrosio et al., MACRO collaboration, Phys. Lett. B434 (1998) 451.

[3] C. Athanassopoulos et al., LSND Collaboration; Phys. Rev. C54 (1996) 2685; Phys. Rev. Lett. 77 (1996) 3082; Phys. Rev. Lett. 81 (1998) 1774.

[4] K. Eitel et al., Nucl. Phys. Proc. Suppl. 70 (1999) 210.

[5] M. Gell-Mann, P. Ramond and R. Slansky, proceedings of the Supergravity Stony Brook Workshop, New York, 1979, eds. P. Van Nieuwenhuizen and D. Freedman (North-Holland, Amsterdam).

[6] The literature on the subject is vast. Some indicative references are: C.D. Froggatt and H.B. Nielsen, Nucl. Phys. B147 (1979) 277; H. Fritzsch, Phys. Lett. 70B (1977) 436; B73 (1978) 317; Nucl. Phys. B155 (1979) 189; C. Wetterich, Nucl. Phys. B261 (1985) 461; G.K. Leontaris and D.V. Nanopoulos, Phys. Lett. B212 (1988) 327.

[7] L. Ibanez and G.G. Ross, Phys. Lett. B332 (1994) 100; Y. Grossman and Y. Nir, Nucl. Phys. B448 (1995) 30; P. Binétruy, S. Lavignac and P. Ramond, Nucl. Phys. B477 (1996) 353; H. Dreiner et al., Nucl. Phys. B436 (1995) 461; G.K. Leontaris, S. Lola and G.G. Ross, Nucl. Phys. B454 (1995) 25; S. Lola and G.G.Ross, hep-ph/9902283.

[8] J. Ellis, G.K. Leontaris, S. Lola and D.V. Nanopoulos, hep-ph/9808251, to appear in Eur. J. Phys. C; J. Ellis, S. Lola and D.V. Nanopoulos, hep-ph/9902364.

[9] See for example G. Altarelli and F. Feruglio, Phys. Lett. B439 (1998) 112; JHEP 9811 (1998) 021; hep-ph/9812475 and references therein.

[10] G.K. Leontaris, S. Lola, C. Scheich and J.D. Vergados, Phys. Rev. D 53 (1996) 6381; S. Lola and J.D. Vergados, Progr. Part. Nucl. Phys. 40 (1998) 71.

[11] V. Barger et al., hep-ph/9810121; G.L. Fogli et al., hep-ph/9902267.

[12] M.C. Gonzalez-Garcia et al., hep-ph/9809531.

[13] M. Carena, D. Choudhury, S. Lola and C. Quigg, Phys. Rev. D58 (1998) 095003.

[14] For recent reviews, see G. Bhattacharyya, hep-ph/9709395; H. Dreiner, hep-ph/9707435.

[15] R. Gandhi et al., Astropart. Phys. 5 (1996) 81.

[16] H. Lai et. al., CTEQ Collaboration, Phys. Rev. D51(1995) 4763.